Vol. 16(4), pp. 188-195, October-December, 2021
DOI: 10.5897/IJPS2021.4970
Article Number: 2382B7868440
ISSN 1992-1950

http://www.academicjournals.org/IJPS

International Journal of Physical Sciences

Full Length Research Paper

Theoretical and experimental studies of effective carriers lifetime: Magnetic effects

SAM Raguilignaba[1,2], DIASSO Alain[2*], ZOUMA Bernard[3] and ZOUGMORÉ François[2]

[1]Units of Sciences and Technology, Department of Physics, Laboratory of Heliophysic, Materials and Environment, Nazi Boni University, Bobo Dioulasso, Burkina Faso.
[2]Units of Sciences and Technology, Department of physics, Laboratory of Materials and Environment, Joseph Ki-Zerbo University, Ouagadougou, Burkina Faso.
[3]Units of Sciences and Technology, University of Ouagadougou, Department of Physics, Laboratory of Thermal and Renewable Energy, Ouagadougou, Burkina Faso

Received 4 October, 2021; Accepted 22 December, 2021

In this manuscript, we present a study on the effects of magnetic field on charge carrier effective lifetime within the base of a polycrystalline PV solar cell p-n junction. This study is elaborated in two forms as a theoretical study and an experimental study. Indeed, under various magnetic field values, PV solar cell is illuminated by using the light from stroboscopic. From a theoretical approach mainly use the open circuit voltage decay method. Green's functions and boundaries conditions are used to solve charge carrier's diffusion equation. Open circuit transient voltage decay expression is found. The charge carriers' effective lifetime values inversely proportional to the slope of open circuit voltage decay curve are deducted. A simple experimental set-up used open circuit voltage decay method mainly, these experimental measurements of charge carriers' effective lifetime are done and the effects of magnetic field are then outlined. Globally, magnetic effects on effective charge carrier lifetime are then analyzed. These two types of results obtained present qualitatively the decay of charge carriers' effective lifetime when magnetic field increase. In the first time, theoretical results and experimental results are in good agreement and in the second time these results are in good agreement with literature results.

Key words: Effective lifetime, open circuit voltage decay, magnetic field.

INTRODUCTION

Minority charge carrier effective lifetime is an important parameter to estimate the quality of a PV solar cell. Indeed, the overall energy conversion efficiency of a photovoltaic cell is based on minority charge carrier's effective lifetime of PV solar cell. So, more methods are been developed for effective lifetime measurement (Dhariwal and Vasu, 1981; Mahan et al., 1979). Among these methods, open-circuit voltage decay is a simple and reliable technic to measure the minority charge carrier's effective lifetime in PV solar cell. Since then, both theoretical and experimental investigations on the application of this method to the characterization of

*Corresponding author. E-mail: alinodiass@yahoo.fr.

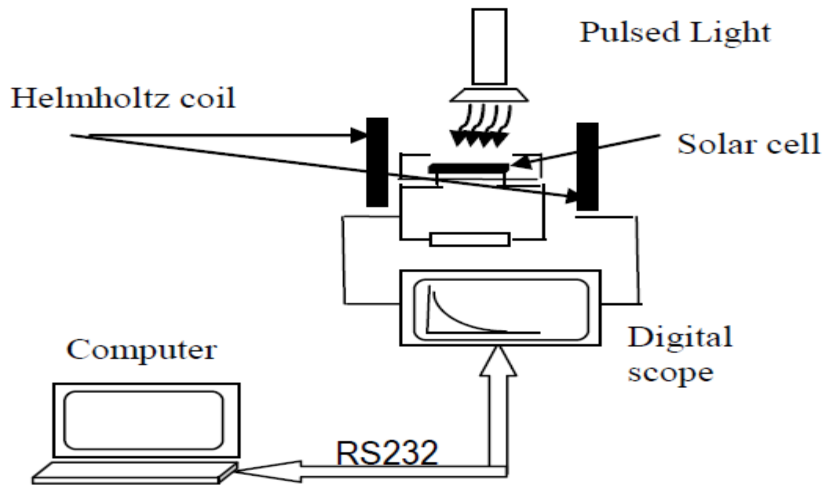

Figure 1. Experimental set-up (Sam et al., 2012).

photovoltaic devices have been discussed and the technic extended (Jain, 1981; Agarwal et al., 1982).

In this manuscript, we present a technic to measure charge carrier effective lifetime of PV solar cell method. This method mainly used open circuit voltage decay conditions. Firstly, experimental set-up is presented, study assumptions are made and experimental conditions are described. Secondly, in this study, new analytical expressions of excess minority charge carrier density and transient open circuit voltage were determined from mathematical formulation. Thirdly, theoretical and experimental results on charge carrier effective lifetime in a polycrystalline silicon p-n junction under magnetic field are found and analyzed. The effects of magnetic field on effective charge carrier lifetime are then analyzed.

MATERIALS

The list of experimental set-up material is as followed: A mono-facial silicon solar cell manufactured by MOTCH INDUSTRY; a pulsed light source MINISTROB PHIWE, a digital oscillo-scope TECKTRONIX model TDS 10013, a computer INTEL 586, a power supply 0-12V DC/ 6V-12V AC , a tesla meter and Helmholtz Coil. The experimental set-up is presented on Figure 1.

The experimental system principle operating is identical than that described by Sam et al. (2012, 2016). In addition, the stroboscopic flash used is considered near AM1.5. Also, any external or internal factors which can perturb PV solar cell operating conditions were neglected (Ba and Kane, 1995).

At time t=0, the PV cell is illuminated with the multispectral flash which establishes a steady state characterized by the potential V_2 corresponding to an operating point called 2 (Figure 2). At time t=Te, the flash is abruptly cut off. The voltage V_2 drops from V_2 to V_1 corresponding to a new operating point denoted 1. The decay of voltage from V_2 to V_1 is recorded on a digital scope connected to an external hard drive.

External hard drive permits to save experimental data for the rebuilding of the signal response later. Kaleidagraph software is used to convert complex data obtained during experimentation into transient voltage graphs.

METHODS

A bifacial polycrystaline solar cell operating under a various magnetic field was considered. This PV solar cell, because of its manufacture technic, is constituted of several grains of different sizes and forms separated by grain boundaries that are considerable recombination centers. For the modeling of the processes of generation, diffusion, and recombination, the polycrystalline, PV solar cell was considered as a regular array of many unit cells with dimensions 2a, 2b and H (Figure 3). This modeling of polycrystalline solar cell structure was described in detail by the authors of references (Ba et al., 1993; Diasso et al., 2020a; Charles et al., 2000; Toure et al., 2012). With this hypothesis, the properties of polycrystalline solar cell can be described by a study of generation, diffusion, and recombination processes only in one grain. Figure 3 shows the theoretical model for a sample grain. The following assumptions for this study to solve diffusion equation are:

1. The emitter and space charge region contributions are neglected to the photocurrent production, so the majority of the current is provided therefore by the base (Diasso et al., 2020d; Dieng and al, 2011; Mohammad, 1987).
2. The grains are under parallelepipedic shape (2a 2b and H) and the joints of the grains are perpendicular to the junction (Mohammad, 1987).
3. The surfaces between two adjacent grains and perpendicular to the junction are characterized by the same carrier recombination process evaluated by a grain boundary recombination velocity (Mohammad, 1987):

$$Sgx = Sgy = Sg \tag{1}$$

The magnetic field is oriented according to the direction $\overrightarrow{oy}$, $\vec{B} = B\overrightarrow{oy}$. It is therefore perpendicular to the depth of light penetration in order to observe the effect of the strength of Lorentz on the charge carriers;
4. The solar cell is uniformly. Then, we have a generation rate

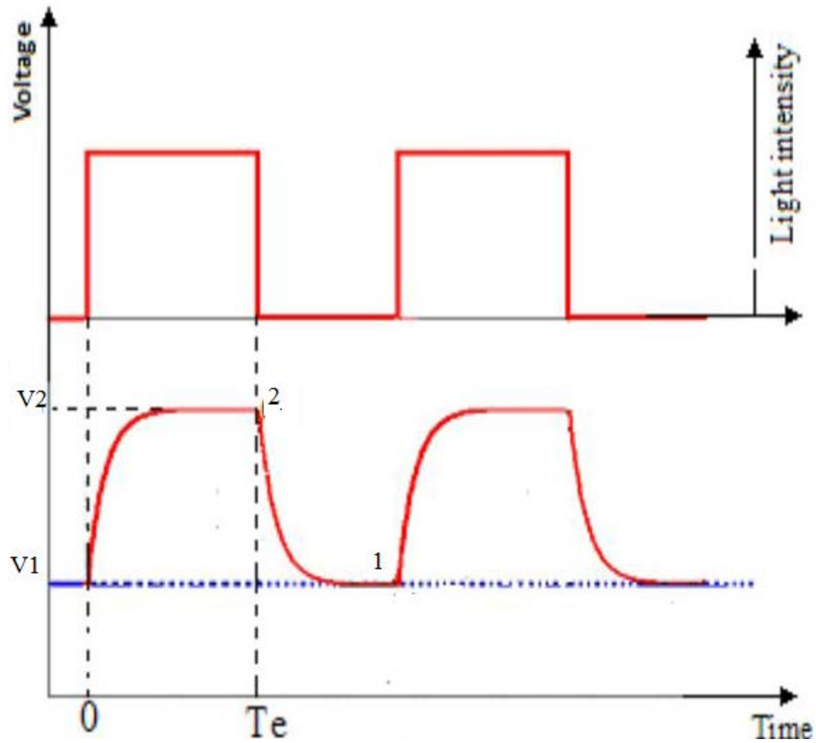

Figure 2. Operating mode.

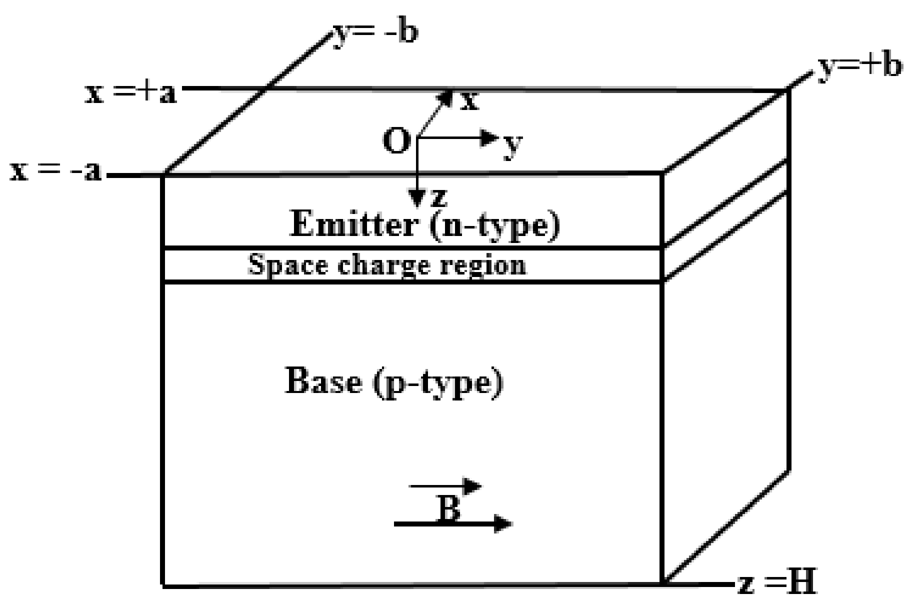

Figure 3. A theoretical model of grain with external magnetic field.

depending only on the depth in the base z;

5. The insulation level number (sun number) $n = 1$.

In the base, the minority charge carriers are electrons, and charge carriers density expression is given by the resolution of the Equation 2:

$$\frac{\partial \delta n}{\partial t} = \frac{1}{e}\vec{\nabla}.\vec{j}_n + g_n - r_n \quad (2)$$

g_n , r_n are respectively the rate of generation at the distance z and rate recombination of charge carriers. The current density $\vec{j}_n$

expression is:

$$\vec{j}_n = eD_n \vec{\nabla}\delta_n + e\mu_n \vec{E} - \mu_n \vec{j}_n \Lambda \vec{B} \tag{3}$$

$\vec{E}$ is the electric field of the crystal lattice and μ_n is the mobility of the electrons.

Substituting Equation (2) into (1) and taking into account the theory of quasi-neutrality of the base, the diffusion equation of the electrons in the base becomes:

$$\frac{\partial\delta(x,y,z,t)}{\partial t} - D^*\left(\vec{\nabla}\delta(x,y,z,t) - \frac{\delta(x,y,z,t)}{L^*}\right) = g(x,y,z,t) \tag{4}$$

The presence of the magnetic field in our model leads to new values of carrier diffusion length L* and carrier diffusion coefficient D* expressions which depend on the magnetic field:

$$D^* = \frac{D}{\theta} \tag{5}$$

Magnetic field intensity is as a function of coefficient θ.

The carriers' generation rate under multispectral light at the depth z in the base can be written by Expression 6:

$$g(z,t) = \begin{cases} \sum_{n=1}^{3} a_m \exp(-b_m z) \text{ si } 0 \le \text{t} \le \text{Te} \\ 0 \qquad \text{si } t \succ Te \end{cases} \tag{6}$$

In this equation, coefficients a_m and b_m are the modeling coefficients of AM1.5 (Ba and Kane, 1995). Equation (1) is solved with the following boundaries conditions:

At junction z = 0

$$\left.\frac{\partial\delta(x,y,z,t)}{\partial z}\right|_{z=0} = \frac{Sf}{D^*}\delta(x,y,z=0,t) \tag{7}$$

At rear side z = H

$$\left.\frac{\partial\delta(x,y,z,t)}{\partial z}\right|_{z=H} = \frac{Sb}{D^*}\delta(x,y,z=H,t) \tag{8}$$

At surfaces limited by $x = \pm a$ and $y = \pm b$

$$\left.\frac{\partial\delta(x,y,z,t)}{\partial x}\right|_{x=\pm a} = \pm\frac{Sgx}{D^*}\delta(x=\pm a,y,z,t) \tag{9}$$

$$\left.\frac{\partial\delta(x,y,z,t)}{\partial y}\right|_{y=\pm b} = \pm\frac{Sgy}{D^*}\delta(x,y=\pm b,z,t) \tag{10}$$

Sf, Sb and Sg are recombination velocity of minority charge carriers respectively at surfaces $z = 0$, $z = \text{H}$ and $x = \pm a$ (or $y = \pm b$). a, b and H are the grain sizes as indicated on Figure 1.

A solution of Equation (1) is expressed according to Ba and Kane (1995).

$$G = \sum_{i=1}^{+\infty}\sum_{j=1}^{+\infty}\sum_{k=1}^{+\infty} P_i P_j P_k \exp\left(-\beta\left(t-t'\right)\right) \tag{11}$$

Where:

$$P_i = A^2_{k_i}\cos\left(k_i x'\right)\cos\left(k_i x\right) \tag{12}$$

$$P_j = A^2_{l_j}\cos\left(l^*_j y'\right)\cos\left(l^*_j y\right) \tag{13}$$

$$P_k = A^2_{\mu_k}\cos\left(\mu_k z' + \varphi_k\right)\cos\left(\mu_k z + \varphi_k\right) \tag{14}$$

β^* and l_j^* are expressed by:

$$\beta^* = D^*\left(k^2{}_i + l^2{}_j + \mu^2{}_k + \frac{1}{L^{*2}}\right) \tag{15}$$

$$l^*{}_j = \frac{l_j}{\sqrt{\theta}} \tag{16}$$

The expression (11) can write simply by the following equation:

$$\delta_1(x,y,z,t) = \left[\begin{array}{c} \dfrac{B\sin(k_{i,1}a)\sin(\frac{l_{j,1}}{\sqrt{\theta}}b)}{k_{i,1}\frac{l_{j,1}}{\sqrt{\theta}}\beta^*}K \\ \times\cos(k_{i,1}.x).\cos(\frac{l_{j,1}}{\sqrt{\theta}}y)\cos(\mu_{k,1}z+\varphi_{k,1}) \end{array}\right].F_0(t) \tag{17}$$

is the expression of carriers density. Where:

$$B = 4.n.a_m.A^2_{k_{i,1}}.A^2_{l_{j,1}}.A^2_{\mu_{k,1}}$$

$$F_0(t) = \left(1-\exp(-\beta^* Te)\right).\exp(-\beta^*(t-Te) \tag{18}$$

$$K = \frac{a_m.b_m}{b_m{}^2+\mu_k{}^2}\left[\begin{array}{l} -\exp(-b_m.H)\cos(\mu_k.H+\varphi_k)+\cos(\varphi_k)+ \\ \dfrac{\mu_k}{b_m}\exp(b_m.H)\times\sin(\mu_k.H+\varphi_k)-\dfrac{\mu_k}{b_m}\sin(\varphi_k) \end{array}\right] \tag{19}$$

The values of A_{l_i}, A_{l_j} and A_{μ_k} are obtained by normalizing P_i, P_j and P_k.The parameters k_i, l_j and μ_k are the Eigen values obtained from the boundaries conditions. φ_k is the initial phase and is determined by solving the Equation 20:

$$\tan\left(\mu_k H + \varphi_k\right) = \frac{Sb}{\mu_k D^*} \quad (20)$$

The transient open circuit voltage decay is given by Equation 21:

$$V\left(t\right) = V_T Fv\left(k_1; l^*{}_1; \mu_1\right) r \exp\left(-\beta\left(t - Te\right)\right) \quad (21)$$

where $r = \exp(\frac{\Delta V}{V_T}) - 1$ and $\Delta V = V_O - V_F$ (22)

$$Fv(k_1, l^*{}_1, \mu_1) = \frac{\Delta_0(0,0)}{\Delta(0,0)} . \left[1 - \exp\left(-\beta^* . Te\right)\right] \quad (23)$$

The quantities $\Delta_0\left(0,0\right)$ and $\Delta\left(0,0\right)$ are defined by:

$$\Delta_0\left(0,0\right) = \int_{-a}^{a}\int_{-b}^{b} Z_{111}\left(x,y,0\right) dxdy \quad (24)$$

$$\Delta\left(0,0\right) = \int_{-a}^{a}\int_{-b}^{b} d_{111}\left(x,y,0\right) dxdy \quad (25)$$

$Z_{111}\left(x,y,0\right)$ and $d_{111}\left(x,y,0\right)$ are respectively the spatial component of $\delta\left(x,y,z,t\right)$ and the minority carrier density during illumination phase.

$$l^*{}_1 = \frac{l_1}{\sqrt{\theta}} \quad (26)$$

According to expression (21), we have two types of open circuit voltage decay:

if $Fv\left(k_1; l^*{}_1; \mu_1\right) r \exp\left(-\beta^*\left(t - Te\right)\right) \prec\prec 1$

The time dependent open voltage decay become:

$$V\left(t\right) = V_T\left[-\beta^*\left(t - Te\right) + \ln\left(1 + Fv\left(k_1; l^*{}_1; \mu_1\right)\right) r\right] \quad (27)$$

This expression of transient voltage is a linear function of the time with a negative slope $-V_T\beta^*$ if $Fv\left(k_1; l^*{}_1; \mu_1\right) r \exp\left(-\beta^*\left(t - Te\right)\right) \prec\prec 1$

Samply, $V(t)$ becomes:

$$V\left(t\right) = V_T Fv\left(k_1; l^*{}_1; \mu_1\right) r \exp\left(-\beta\left(t - Te\right)\right) \quad (28)$$

$V(t)$ is a time dependent decay exponential function.

RESULTS AND DISCUSSION

Effective lifetime of minority charge carriers' measurement

The approach employed in the study is based on the linear approximation of the transient voltage decay because in low injection there are no impedance effects (Muralidharan and Jain, 1982). Figure 4 presents the different regions of transient voltage decay curve.

The linear decay zone of the curve was identified, then, a fit was applied on this zone and a linear regression line was obtained with it equation expression illustrated by Figure 5. In Figure 5, the linear regression equation is established with a good correlation coefficient R. The slope m of this linear regression line is related to the effective lifetime of minority charge carriers by expression 28.

$$\left|m\right| = \frac{V_T}{\tau_{eff}} \quad (28)$$

m is the slope of transient voltage decay curve, V_T is the thermic voltage, and τ_{eff} indicates charge carrier effective lifetime value.

Magnetic effects on effective carriers lifetime

After registration data with the digital scope, the signal of the transient response was remade. Then, the curves of transient voltage decay were gotten for various magnetic field values. Just one example of the transient voltage curves obtained was shown here (Figure 6). The figure shows two forms of decay: Linear decay and exponential decay. After analysis, it is indicated that the linear region is major than the linear zone (75 against 25%). Ideal types of open circuit transient voltage decay according to Dhariwal and Vasu (1981) and Mahan et al. (1979) was gotten. Additionally, this zone of the curve doesn't present capacitance effects in reference to Dhariwal and Vasu (1981), Mohammad (1987) and Diasso et al. (2020b).

Theoretical results

The theoretical results obtained from a linear fit are given in Table 1. The observation of the precedent table of theoretical results shows the decrease in charge carrier's effective lifetime is a function of magnetic field.

Experimental results

The experimental results of all transient voltage decay

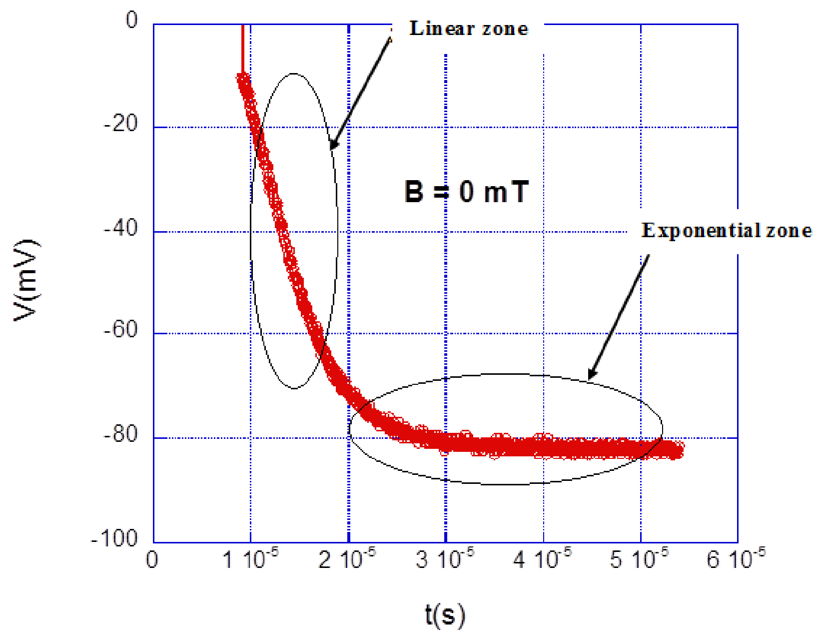

Figure 4. Different regions of transient voltage decay.

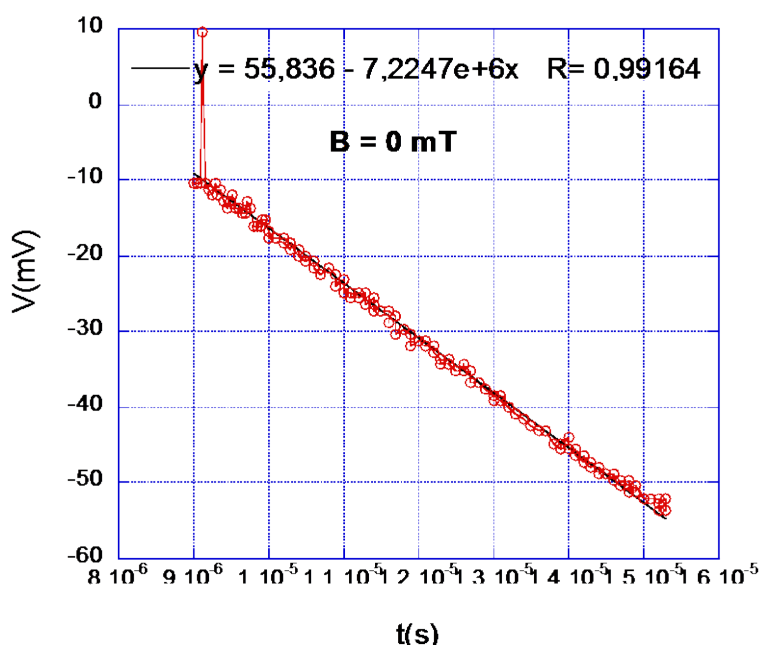

Figure 5. A linear regression line with it equation.

curves linear fitting obtained are given in Table 2.

We remark that the results indicate the decrease of charge carrier's effective lifetime theoretical or experimental values versus magnetic field.

The analysis of the two types of results present a decrease in effective charge carrier's lifetime with the increase in magnetic field.

The increase in magnetic field creates the decrease in diffusion length and diffusion coefficient. This reduction of diffusion length and diffusion coefficient induce fast minority charge carriers' recombination reducing distance and time during recombination when the magnetic field increases. Also, the extension of space charge region width is, an increase in a function of magnetic field

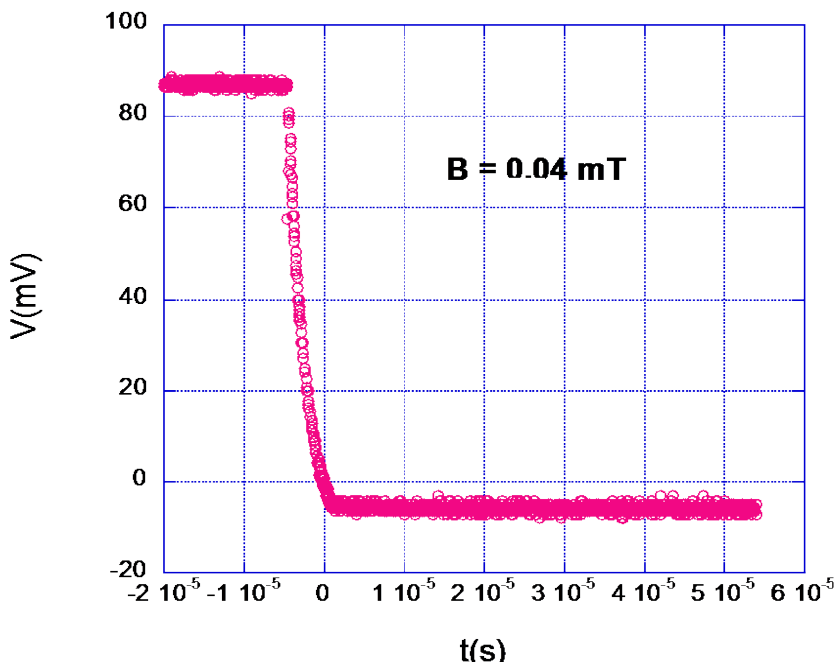

Figure 6. Transient voltage decay B=0.040 mT.

Table 1. Theoretical effective lifetime value versus magnetic field values.

Magnetic values, B (mT)	**0**	**0.02**	**0.03**	**0.05**	**0.07**	**0.08**	**0.10**	**0.12**
Effective Lifetime (µs)	4.33	4.26	4.22	4.14	4.03	3.71	3.46	3.25
Corelation coefficient R	0.98	0.96	0.97	0.97	0.95	0.98	0.96	0.99

Table 1. Experimental effective lifetime values versus magnetic field values.

B (mT)	0	0.010	0.015	0.020	0.030	0.035	0.040	0.045
$\tau_{effL}\,(\mu s)$	3.60	3.60	3.32	3.24	1.02	1.01	1.00	1.00
R_E	0.99	0.99	0.98	0.96	0.96	0.97	0.98	0.94

traduces an important disappearance of charge carriers and therefore the strong reduction of effective charge carriers lifetime. The comparison of theoretical results and experimental results show the decay of the charge carries effective lifetime with the increase of magnetic field. So the two types of results are in good agreement qualitatively.

Conclusion

In this paper, theoretical study and experimental study were conducted. For this study, the theoretical approach and the experimental set up are presented. The list of experimental set-up material and experimental conditions are described. Firstly, theoretically, a three dimensional approach of electrons diffusion in the p region of a polycrystalline silicon solar cell is presented when solar cell is front side illuminated by a pulsed light versus external magnetic field. The expressions of charge carriers density and transient voltage decay are established. Secondly, we pointed out a simple and reliable experimental and theoretical technic to measure effective charge carriers' lifetime. Thirdly, the effects of magnetic field on charge carriers' effective lifetime are presented and analyzed.

CONFLICT OF INTERESTS

The authors have not declared any conflict of interests.

REFERENCES

Agarwal SK, Jain SC, Harsh S (1982). Variation of minority carrier lifetime with level of injection in pn-junction devices. Electronics Letters 18(7):298-299.

Ba B, Kane M (1995). Open-circuit voltage decay in polycrystalline silicon solar cells. Solar Energy Materials and Solar Cells 37(3-4):259-271.

Ba B, Kane M, Fickou A, Sissoko G (1993). Excess minority carrier densities and transient short circuit currents in polycrystalline silicon solar cells. Solar Energy Materials and Solar Cells 31(1):33-49.

Charles JP, Haddi A, Maouad A, Bakhtiar H, Zerga A, Hoffmann A, Mialhe P (2000). La jo nction, du solaire à la microélectronique. Reviews Energy Renewable 3:1-16

Dhariwal SR, Vasu NK (1981). A generalised approach to lifetime measurement in pn junction solar cells. Solid-State Electron 24(10):915-927.

Diasso A, Raguilignaba S, François Z (2020). Research Journal of Applied Sciences, Engineering and Technology 17(4):140-146, DOI: 10.19026-rjaset.17.6026.

Diasso A, Sam R, Zouma B, François Z (2020a). Experimental Measurement of Minority Carriers Effective Lifetime in Silicon Solar Cell Using Open Circuit Voltage Decay under Magnetic Field in Transient Mode. Smart Grid and Renewable Energy 11(11):181-190. DOI: 10.4236-sgre.2020.1111011

Diasso A, Sam R, Traoré NY, Zougmoré F (2020b). Effects of External Magnetic Field and Air Mass on Space Charge Region Width Extension of a Bifacial Solar Cell Front Side Illumination. International Journal of Energy and Power Engineering 9(3):29-34. doi:10.11648/J.ijepe. 20200903. 11

Dieng A, Zerbo I Wade M, Maiga AS, Sissoko G (2011). Three-dimensional study of a polycrystalline silicon solar cell: The influence of the applied magnetic field on the electrical parameters. Semiconductor Science and Technology 26(9):095023.

Jain SC (1981). Theory of photo induced open circuit voltage decay in a solar cell. Solid-State Electronics 24(2):179-183.

Mahan JE, Ekstedt TW, Frank RI, Kaplow R (1979). Measurement of minority carrier lifetime in solar cells from photo-induced open-circuit voltage decay. IEEE Transactions on Electron Devices 26(5):733-739.

Mohammad SN (1987). An alternative method for the performance analysis of silicon solar cells. Journal of Applied Physics 61(2):767-777.

Muralidharan R, Jain SC (1982). Determination of the minority carrier lifetime in the base of a back-surface field solar cell by forward current-induced voltage decay and photovoltage decay methods. Solar Cells 6(2):162-176.

Sam R, Kaboré K, Zougmoré F (2016). A three-dimensional transient study of a polycrystalline silicon solar cell under constant magnetic field. International Journal of Engineering Research 5(2):93-97. ISSN 2319-6890

Sam R, Zouma B, Zougmoré F, Koalaga Z, Zoungrana M, Zerbo I (2012). 3D determination of the minority carrier lifetime and the pn junction recombination velocity of a polycrystalline silicon solar cell. In IOP Conference Series: Materials Sciences and Engineering 29, doi 10.1088/1757-899X/29/1/012018

Toure F, Zoungrana M, Zouma B, Mbodji S, Gueye S, Diao A, Sissoko G (2012). Influence of Magnetic Field on Electrical Model and Electrical Parameters of a Solar Cell under Intense Multispectral Illumination. International Journal of Advances in Science and Technology 5:40-53.